Molecular dynamics studies of entangled polymer chains

Bulacu, Monica Iulia

Chapter 3

Computational model

All the effects of Nature are only the mathematical consequences of a small number of immutable laws.

Pierre-Simon Laplace

This chapter briefly describes the coarse-grained polymer chain models and the MD technique used to simulate polymeric systems in equilibrium (bulk) or in non-equilibrium conditions (the fracture of the adhesion between two polymer bulks reinforced with connector chains). We start by presenting the advantages of the bead-spring polymer model in the general context of coarse-graining and multiscale modeling. Explicit details are given regarding the implementation of chain characteristics (stiffness along the polymer backbone) in the model used in this thesis. Next, some essential MD features are reviewed from the point of view of their direct implementation in the MD code.

3.1 Molecular dynamics

Molecular dynamics is a specific computer simulation method employed for molecular systems, from ideal gases and liquids to biomolecules and materials (Allen and Tildesley 1987, Haile 1992, Rapaport 2004, Frenkel and Smit 2001). The systems entering molecular dynamics simulations are modeled as ensembles of interacting particles under specific internal and external conditions. Given the initial coordinates and velocities of an ensemble of particles that interact in an explicit manner, under certain conditions, this method integrates the equation of motion numerically, providing new sets of coordinates and velocities at each integration time step. From the obtained particles trajectories one can calculate various global system properties as statistical averages.

Due to the strict control of the internal motion, molecular dynamics is particularly suited for the study of polymeric systems. Polymer macroscopic properties and mechanical response evidently arise from the chain dynamics, primarily governed by segment chain interactions and connectivity. But, unlike ideal systems (gases, liquids or crystals) the chain behavior inside a polymer is extremely complex and still not completely understood theoretically.

3.2 Coarse-grained models for polymers

At first sight, it might be tempting to study, by this technique, dense systems consisting of many long polymer chains, in which all atoms are considered, with detailed chemical interactions, for a long time, to obtain realistic characteristics of the polymer. But such a task would require an exhaustive knowledge of the interaction potentials between all the atomic species considered and a huge computational power that cannot be provided even by the fastest supercomputers. It is therefore imperative to reduce the complexity of the simulated systems in order to perform fruitful simulations.

One elegant way to do this is to group together atoms or monomer units into a bigger chain sub-unit that absorbs all the molecular detail. The new repeat units will feel each other through such interactions as resulted from the realistic replaced parts. Such coarse-graining is suggested by the polymer nature itself: polymers exhibit clear time and length scaling for their static (de Gennes 1979) and dynamic properties (Doi and Edwards 1989); polymers with very different topologies react universally to temperature modifications, some undergoing a similar but "scaled" glass transition (Bulacu and Van der Giessen 2007).

During the past two decades, a variety of coarse-grained models have been proposed for polymers. They mainly differ by the level of discretization for the polymer chain, by how the replaced mass is distributed in the new coarse-grained unit or by the specific

force field used. All these choices are influenced by the final desired tasks, by mapping from atomistic simulations. The various approaches can be classified as follows:

1. United atom

   The united atom model has been developed for *n*-butane by Ryckaert and Bellemans (1975) and then extensively studied (Rigby and Roe 1987, Rigby and Roe 1988, Takeuchi and Roe 1991, Roe 1994). The H atoms in the CH_2 groups are combined in a single unit with the C atom to which they are connected, with the total mass of the H and C atoms located at or near the carbon. A polymer chain is formed by such new units bounded by harmonic springs. The natural stiffness along the chain is modeled by bending and/or torsion potentials. Non-connected beads interact through a Lennard-Jones (LJ) potential.

2. Tangent hard spheres (pearl-necklace)

   The polymer chain is represented by a freely linked chain of hard spheres attached to one another by sliding links connecting their centers. There are no additional angular constraints imposed on adjacent links other than those which are a consequence of the excluded volume (Rapaport 1979, Smith et al. 1996).

3. Ellipsoidal

   This model is suitable for polymers with large or anisotropic monomers in terms of their mass and their non-bonded interactions (e.g. polycarbonate) (Zimmer and Heermann 1995, Schöppe and Heermann 1999). It consists of basic ellipsoidally shaped units stringed together to form chains. The masses of the atoms are smeared out over the principal axes of the ellipsoids yielding a chain with continuous a backbone mass. Harmonic bonds and bending angle potentials are used for the connected ellipsoids while the intermolecular interaction is modeled by non-spherical force fields.

4. Bead–spring

   In this model the chain is reduced to a string of beads, each bead representing one or a few monomer units. The beads along the polymer chain are coupled by a quasiharmonic potential and the repulsive part of the LJ potential is used for the excluded volume. This model has been introduced for the first time in molecular dynamics simulations of a single polymer chain immersed in a solvent by Bishop et al. (1979). Its unquestionable fame has come after the polymer melt simulations of Kremer and Grest (1990). Recently this model has been modified to account also for chain stiffness besides the intrinsic stiffness induced by the excluded volume (Faller and Müller-Plathe 2001, Bulacu and Van der Giessen 2005).

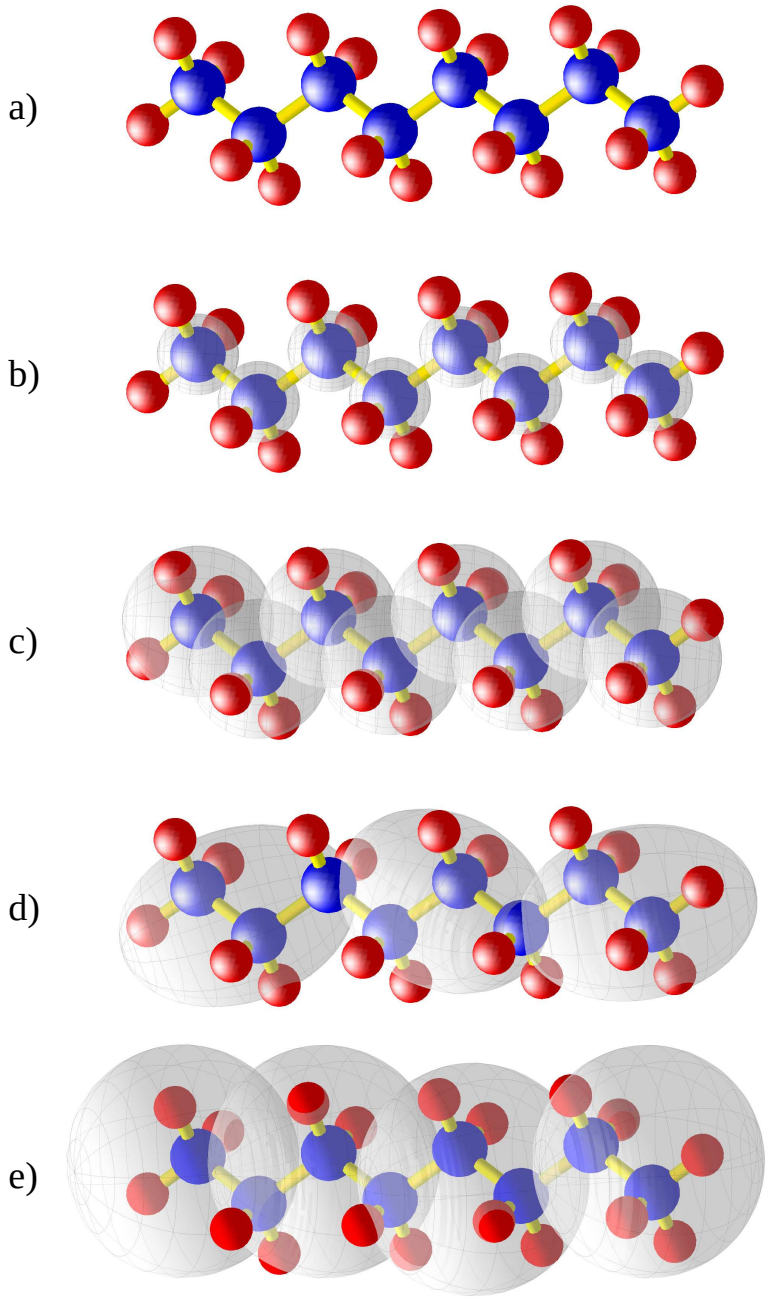

Figure 3.1: *Schematic representation of different levels of coarse-graining for a polymer chain. From top to bottom a polyethylene (PE) chain is represented by: (a) the atomistic model; (b) the united atom model; (c) the tangent hard spheres model; (d) the ellipsoidal model and (e) the bead-spring model.*

The immediate benefits of coarse-grained methods consist in decreasing the number of simulated units and in reducing the complexity of calculations: for example, a polymer chain with 100 atoms of 3 different species can be replaced with a chain of 20 identical coarse-grained beads. This simplification enables further development in two directions: (1) increase in size of the simulated systems: more chains (with direct improvement of the statistics) or longer chains (knowing that the polymer behavior is very much influenced by the chain length); (2) increase of the simulation time to allow polymer equilibration and study of the polymer dynamics behavior. This time expansion is also achievable since larger integration time steps can be used without the MD integrator becoming unstable (the resulting coarse-grained potentials are much softer than atomistic potentials).

As a result, coarse-grained models are very efficient for the study of equilibrated polymeric systems by essentializing the nature of the polymer chain. This thesis presents simulations using a modified bead-spring model, our main interest being to capture the essence of the polymer static and dynamic behavior, rather than to map to a specific polymer. The model that we proposed includes bending and torsion potentials along the backbone to generically control the chain stiffness and to study their influence on polymer characteristics. We have been motivated by recent work of Rapaport (2002) that showed how by controlling the torsion and excluded volume potentials even complicated problems as protein folding can be investigated successfully.

Besides the purely theoretical inquiries, after performing simulations at this mesoscopic level one can map back to atomistic models (by reintroduction of chemical details) and extract the properties of other ways impossible atomistic equilibrated systems (Hess et al. 2006). Other further possibilities are: (1) to map to a higher regime (semi-macroscopic) in which the entire chain is replaced by a big particle, which hides the coarse-grained details, and to perform dissipative particles dynamics (Español 1998); (2) to evaluate specific constants or phenomenological laws for the use at longer length and time scales (up to continuum regime).

The multiscale simulation procedure outlined above is still in the development phase due to the difficulties in performing accurate simulation at one specific level as well as in realistically mapping between the considered scales (Kremer and Müller-Plathe 2001, Kremer and Müller-Plathe 2002). One successful example is the simulation of brittle fracture in silicon by coupling of quantum, atomistic and continuum mechanics (Abraham et al. 1998b, Abraham et al. 1998a, Broughton and Abraham 1999).

Since polymers exhibit various properties on very different length and time scales by their nature, the multiscale modeling of polymeric materials is even more attractive.

3.3 Equation of motion

The conventional MD technique consists in the stepwise time integration of Newton's equations of motion for a set of N particles:

$$\frac{d^2\mathbf{r}_i}{dt^2} = \mathbf{F}_i(\mathbf{r}_1, \mathbf{r}_2, ...\mathbf{r}_N) \tag{3.1}$$

where

$$\mathbf{F}_i(\mathbf{r}_1, \mathbf{r}_2, ...\mathbf{r}_N) = -\nabla_{\mathbf{r}_i} V_i(\mathbf{r}_1, \mathbf{r}_2, ...\mathbf{r}_N) \tag{3.2}$$

Here $\mathbf{r}_i$ is the position vector of the particle i, $\mathbf{F}_i$ is the total force acting on particle i and V_i is the total potential energy from which the force is derived. By solving Newton's equations the total energy of the simulated system is conserved and the time averages obtained during the simulations are equivalent to averages in micro-canonical ensemble i.e. constant–NVE (**n**umber of particles, **v**olume, **e**nergy). But most often this ensemble is not practical when comparing with experimental or theoretical results that traditionally use other ensembles. So, other ensembles are preferred depending on what thermodynamic quantity is kept constant (number of particles, volume, pressure, temperature or chemical potential: canonical ensemble i.e. constant–NVT, isothermal-isobaric ensemble i.e. constant–NPT or grand canonical ensemble i.e. constant–μVT.

All the results presented in this thesis are obtained by performing MD simulations at constant-NVT. One way to obtain this ensemble is by replacing Newton's equations (Eqs. (3.1)-(3.2)) with the Langevin equation:

$$\frac{d^2\mathbf{r}_i}{dt^2} = -\nabla_{\mathbf{r}_i} V_i - \Gamma \frac{d\mathbf{r}_i}{dt} + W_i \tag{3.3}$$

Two additional forces are included in Eq. (3.3) to withdraw/introduce kinetic energy of the system: a frictional force, proportional with the velocity (Γ being the friction constant of the particle) and a stochastic force W. The strength of the noise is related to Γ via the fluctuation dissipation theorem, that is

$$\langle W(t) \rangle = 0 \tag{3.4}$$

$$\langle W_i(t) \cdot W_j(t+\tau) \rangle = 6k_{\mathrm{B}}T\Gamma\delta_{ij}\delta(\tau) \tag{3.5}$$

where $\langle\rangle$ denotes the ensemble's average and δ_{ij} is the Kronecker delta.

3.4 Force field

Understanding the interactions within and between the polymer chains as well as the induced chain topology can help in predicting macroscopic properties of the polymeric

systems. That is why a proper choice of the potentials governing the interactions (force field) is crucial in MD simulations. The forces between particles have to be as realistic as possible and also suitable for feasible simulations since their calculation is the most time consuming part of an MD algorithm.

The most familiar pair interaction potential is the LJ potential:

$$V_{\mathrm{LJ}}(r_{ij}) = 4\varepsilon \left[\left(\frac{\sigma}{r_{ij}} \right)^{12} - \left(\frac{\sigma}{r_{ij}} \right)^{6} \right], r_{ij} < r_{\mathrm{cut-off}}, \tag{3.6}$$

where $r_{ij} = |\mathbf{r}_i - \mathbf{r}_j|$ is the distance between two interacting particles i and j, ε is the minimum energy and σ is the length at which $V_{\mathrm{LJ}}(r_{ij}) = 0$. This potential is characterized by a strong repulsive core ($\propto 1/r^{12}$) and a weak attractive tail ($\propto 1/r^{6}$; the two characteristic powers being used to identify the potential (Eq. (3.6)) as the 12-6 LJ potential. To avoid extensive computation this potential is truncated at a specific distance $r_{\mathrm{cut-off}}$.

This LJ interaction can be simplified by completely neglecting the attractive part: the cut off distance is chosen at the minimum of the V_{LJ} ($r_{\mathrm{cut-off}} = \sqrt[6]{2}\sigma$) and then the potential is shifted such that it vanishes at this distance. The result is known as the Weeks-Chandlers-Andersen, WCA potential (Weeks et al. 1971).

$$V_{\mathrm{WCA}}(r_{ij}) = 4\varepsilon \left[\left(\frac{\sigma}{r_{ij}} \right)^{12} - \left(\frac{\sigma}{r_{ij}} \right)^{6} + \frac{1}{4} \right], r_{ij} < r_{\mathrm{cut-off}}, \tag{3.7}$$

which is plotted in Fig. 3.2 with the gray curve. Particles interacting by this potential act like relatively soft spheres in a narrow range of separation and like hard spheres as they are driven together. The resulting behavior is primarily determined by particle density. For polymeric systems, characterized generally by high particle density, connectivity between beads along the chains and numerous excluded volume interactions, this potential is an excellent choice having a clear advantage in terms of computational simplicity compared with LJ while retaining the essential physics.

The exclusion of the attractive part of the LJ potential requires the use of periodic boundary conditions or impenetrable walls to confine the particle in the simulation box.

One example of an interacting wall is the integrated 9-3 LJ potential (dashed curve in Fig. 3.2). It mimics the interaction of the simulated particles with an infinite half-space uniformly filled with 12-6 LJ particles. Integration over planar sheets of wall atoms results in a perfectly smooth wall, described by the wall potential:

$$V_{\mathrm{LJ}}^{\mathrm{wall}}(z) = \frac{2\pi\varepsilon^{\mathrm{wall}}}{3} \left[\frac{2}{15} \left(\frac{\sigma^{\mathrm{wall}}}{z} \right)^{9} - \left(\frac{\sigma^{\mathrm{wall}}}{z} \right)^{3} \right], z < z_{\mathrm{cut-off}}^{\mathrm{wall}}, \tag{3.8}$$

z being the distance from the wall, and $\varepsilon^{\mathrm{wall}}$ and σ^{wall} allowing the interaction strength of the wall potential to vary.

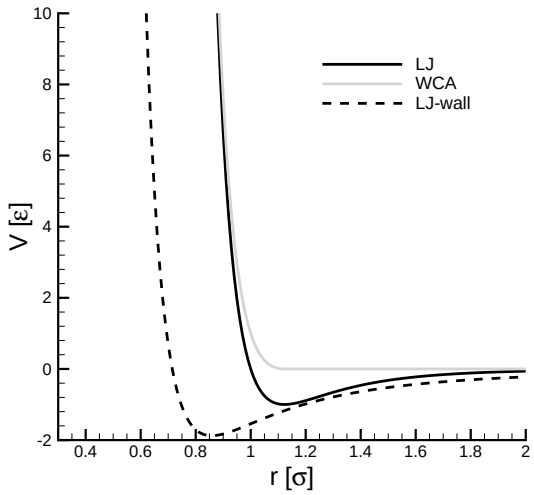

Figure 3.2: *LJ-based potentials: 12-6 LJ (Eq. (3.6)), WCA (Eq. (3.7)) and wall 9-6 LJ (Eq. (3.8)).* r *stands for* r_{ij} *or* z *depending on the potential considered.*

For the chemically bonded beads along the polymer chain a combination of potentials is used: WCA potential (Eq. (3.7)) - to account for the excluded volume interaction, and the attractive Finite Extensible Non-Linear Elastic (FENE) potential - to keep the consecutive beads along the chain bonded together.

The FENE potential is very common in the polymer literature (Warner 1972):

$$V_{\mathrm{FENE}}(r_{ij}) = \begin{cases} -0.5kR^2 \ln\left[1 - \left(\frac{r_{ij}}{R}\right)^2\right], & r_{ij} \leq R_0 \\ \infty\,, \quad r_{ij} > R_0\,. \end{cases} \tag{3.9}$$

it has the form of a simple harmonic potential for small extensions $r_{ij}/R_0 < 0.2$ and limits the spring extensibility to R_0.

Superposition of the FENE and WCA potentials (the dashed curve in Fig. 3.3), with specific parameter values, yields an anharmonic spring interaction between connected beads with an equilibrium bond length b_0 and an ultimate bond length $r_{\max}$. As a consequence, bond crossing in systems of polymer chains is energetically unfavorable and chain entanglement is naturally obtained (Kremer and Grest 1990).

The resulting bond length distribution induced by these potentials is asymmetric: longer bonds are more favorable than short bonds. This becomes a disadvantage when we perform adhesion studies where the elongation of the bonds is considered a measure of the tension induced mechanically from exterior. This can be overcome by a modified form of FENE, i.e. reflected FENE:

$$V_{\mathrm{RFENE}}(r_{ij}) = \begin{cases} -0.5 k_r R_r^2 \ln\left\{\left[1-\left(\frac{r_{ij}}{R_r}\right)^2\right]\left[1-\left(\frac{2\sigma-r_{ij}}{R_r}\right)^2\right]\right\}, & r_{ij} \le R_r \\ \infty, & r_{ij} > R_r\,. \end{cases} \tag{3.10}$$

The parameters k_r and R_r are chosen in such a way that this potential reproduces the result of the FENE + WCA potential for the region of short and middle size bonds while being symmetric over the complete bond length interval.

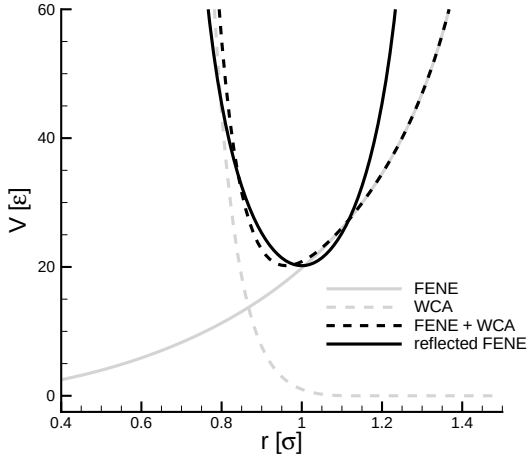

Figure 3.3: *Bond potentials: FENE + WCA (black dashed line) and reflected FENE (black solid line).*

The stiffness of polymer chains can be controlled by a bending potential V_B, which acts on three consecutive beads along the chain. The angle between adjacent pairs of bonds is maintained close to the equilibrium value $\theta_0 = 109.5^\circ$ by the cosine harmonic bending potential (Fig. 3.4):

$$V_\mathrm{B}(\theta_i) = \frac{1}{2} k_\theta (\cos\theta_i - \cos\theta_0)^2, \tag{3.11}$$

where θ_i is the bending angle between bonds b_{i-1} and b_i. The value of the bending constant k_θ is varied to obtain different chain stiffness with the corresponding characteristic ratios.

Further stiffness can be introduced by a torsion potential V_T acting on four consecutive beads (Fig. 3.5). This potential mainly constrains the dihedral angle ϕ_i, which is defined by three successive bonds, b_{i-2}, b_{i-1} and b_i. In this thesis, we use the novel torsion potential (Bulacu and Van der Giessen 2005):

$$V_\mathrm{T}(\theta_{i-1}, \theta_i, \phi_i) = k_\phi \sin^3\theta_{i-1} \sin^3\theta_i \sum_{n=0}^{3} a_n \cos^n\phi_i. \tag{3.12}$$

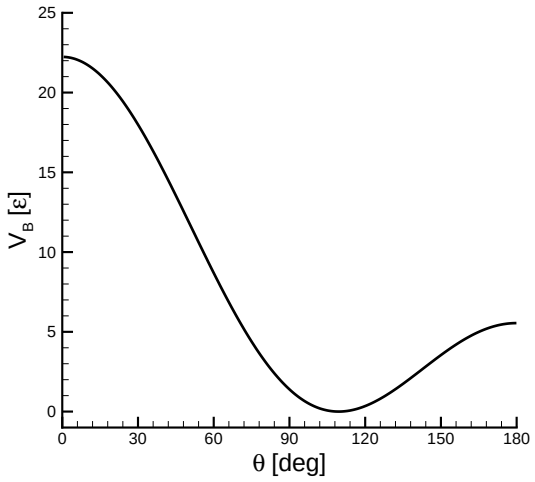

Figure 3.4: *Bending potential V_{B} acting on the bending angles θ with the equilibrium value at $\theta_0 = 109.5°$.*

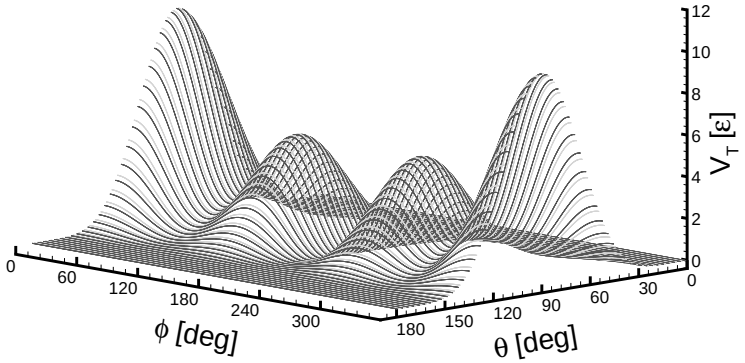

Figure 3.5: *Surface plot of the torsion potential (Eq. (3.12)) when, for simplicity, $\theta_{i-1} = \theta_i = \theta$.*

This potential not only depends on the dihedral angle ϕ_i but also on the bending angles θ_{i-1} and θ_i formed by the three successive bonds. The third-order polynomial in $\cos\phi_i$ follows from *ab initio* calculations for n-butane (Steele 1985). It has three minima for $\phi = 180°$ (trans), $\phi = 60°$ (gauche$^+$) and $\phi = 300°$ (gauche$^-$). The two $\sin^3\theta$ prefactors, tentatively suggested by Scott and Scheraga (1966) and theoretically discussed by Pauling (1960), cancel the torsion potential and force when either of the two bending angles vanishes, which would make the dihedral angle ϕ undefined. This important property makes the potential well-behaved for MD simulations that have no rigid constraints on the bending angles; torsion potentials that are independent of the bending angles suffer from the problem that the torsion forces tend to infinity when two consecutive bonds are aligned. A strong bending potential may prevent this tendency, but

when bonds do align the simulation breaks down. The torsion potential proposed here gracefully eliminates these singularities and improves numerical stability.

It is important to note that the bending and torsion potentials together form a combined potential $V_{\mathrm{CBT}} = V_{\mathrm{B}} + V_{\mathrm{T}}$ that determines the dynamics of the polymer chain. V_{CBT} induces a new equilibrium bending angle θ_{eq} that is slightly larger than θ_0 resulting from V_{B} only, while the equilibrium torsion angles are identical with those induced by V_{T}. The average bond length is not affected by including stiffness along the chain.

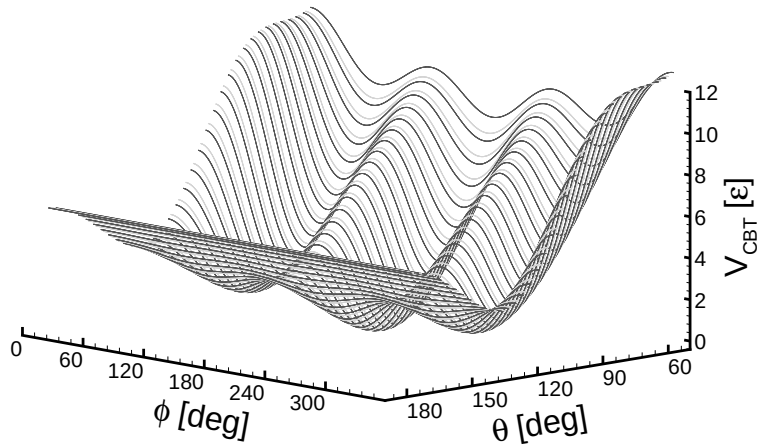

Figure 3.6: *Surface plot of the combined bending-torsion potential $V_{\mathrm{CBT}} = V_{\mathrm{B}} + V_{\mathrm{T}}$ when $\theta_{i-1} = \theta_i = \theta$ is considered. The chain conformation during dynamics will evolve towards the three local minima.*

3.5 LJ units

The physical quantities of interest cannot be expressed directly in international system of units (SI) during MD simulations. Their numerical values would be either very small or very large and thus can lead to overflow or underflow as a result of floating-point operations. It is therefore necessary and elegant at the same time, to represent all quantities in units such that their numerical values are around the value 1.0. When using the Lennard-Jones potential in simulations, its parameters σ and ε are without doubt the most appropriate units of length and energy ($\sigma = 1.0$, $\varepsilon = 1.0$). These, together with the bead mass $m = 1.0$, become the basic MD units, while the rest of physical quantities are expressed in derived units.

Table 3.1 gives such examples of some physical quantities of interest in LJ units and in SI units (for the case in which the bead is the CH_2 unit of polyethylene or a possible group of polymer units). The Boltzmann's constant is considered also $k_{\mathrm{B}} = 1.0$.

Physical quantity	LJ unit	SI unit for CH_2	SI unit for a possible Kremer-Grest model
length	σ	0.38 nm	0.50 nm
energy	ε	0.83×10^{-21} J	4.8×10^{-21} J
mass	m	14 g/mol	289 g/mol
time	$\sigma(m/\varepsilon)^{1/2}$	2.01 ps	5.0 ps
temperature	$\varepsilon/k_{\mathrm{B}}$	60.4 K	347.9 K
pressure	ε/σ^3	15.13 MPa	38.4 MPa
velocity	$(\varepsilon/m)^{1/2}$	1.89×10^2 m/s	1.0×10^2 m/s
force	ε/σ	2.18×10^{-12} N	9.6×10^{-12} N
number density	$1/\sigma^3$	18.22 nm^{-3}	8 nm^{-3}

Table 3.1: *Some physical quantities of interest expressed in Lennard-Jones reduced units and in SI units.*

The bridge between computer simulations and experimental results remains a difficult and controversial task. The link between the MD units and the SI units cannot be established in absolute terms and only the order of magnitude of this relationship is more certain. Nevertheless, it is important to observe that the predictions obtained from computer simulations remain valuable as to what regards the general scaling laws and overall behavior of the statistical ensemble of interacting particles. Furthermore, the computational model represents an interesting object of study in itself, because the insights obtained from simulations can lead to a better understanding of the real physical processes, even if the numerical predictions are difficult to correlate with result obtained in the laboratory.

3.6 Integration scheme

Newton's equations of motion are integrated by means of the 'velocity-Verlet' integration scheme (Swope et al. 1982). The position and velocity of each particle from the system are updated from time t to time $t + \Delta t$ using an intermediate half time-step at $t + \frac{1}{2}\Delta t$:

$$\mathbf{r}(t + \Delta t) = \mathbf{r}(t) + \mathbf{v}(t)\Delta t + \frac{1}{2}\mathbf{a}(t)\Delta t^2 \tag{3.13}$$

and

$$\mathbf{v}(t + \frac{1}{2}\Delta t) = \mathbf{v}(t) + \frac{1}{2}\mathbf{a}(t)\Delta t. \tag{3.14}$$

Using the updated positions and velocities from Eq. (3.13) and Eq. (3.14), the force $\mathbf{F}(t+\Delta t)$ is evaluated. Since we are integrating Newton's equations, $\mathbf{a}(t+\Delta t)$ is just the force divided by the mass and than the final velocity is computed as:

$$\mathbf{v}(t+\Delta t) = \mathbf{v}(t+\frac{1}{2}\Delta t) + \frac{1}{2}\mathbf{a}(t+\Delta t)\Delta t. \tag{3.15}$$

This integrator is fast, simple and stable and, more importantly, it satisfies the requirements of time-reversibility and area conservation (simplectic algorithm) (Frenkel and Smit 2001).

3.7 Thermostats

Solving the Langevin equations Eq. (3.3) with conditions (Eqs. (3.4) and (3.5)) the MD simulations sample the canonical ensemble by keeping the system temperature constant at a desirable value T. This method is known also as the Langevin thermostat and reflects the weak coupling of each particle with a virtual heat bath represented by the combination of frictional and random forces (Grest and Kremer 1986).

A Langevin thermostat has two major advantages that make it very suitable for simulating polymeric materials for which long simulation time is needed. One is that it accepts larger time steps than other thermostats without causing instabilities. The other is that by coupling the system to the background, the inevitable effect of accumulating numerical errors is diminished with the direct consequence of improving the systems' stability over long runs.

Due to the random forces, however, the center of mass of the entire system will drift. This has to be removed for the subsequent analysis of the internal motion. After this correction the long-time diffusion is equivalent with one obtained by using the Berendsen thermostat (which conserves also the momentum but has the disadvantage that it is unknown if it generates an ensemble) (Berendsen et al. 1984). To show this, Fig. 3.7 includes the results for the mean-square displacements g_1, g_2 and g_3 from simulations of identical systems using Langevin or Berendsen thermostats. This similarity appears because the simulated systems are very dense and the diffusion is dependent only on the interactions between constitutive particles and does not arise from the extra Langevin terms: the observed particle friction coefficient is much larger than the Langevin friction coefficient (Kremer and Grest 1990).

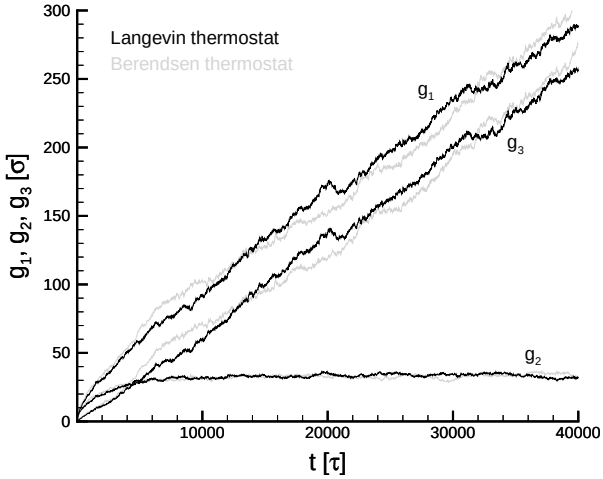

Figure 3.7: *Comparison between the computed mean-squared displacements g_1, g_2 and g_3 for a system with $M = 100$ FJC chains with $N = 50$ beads per chain at $T = 1\varepsilon/k_{\mathrm{B}}$ obtained from simulations using Langevin (black lines) and Berendsen (gray lines) thermostats.*

3.8 Sample initialization

In this thesis we present simulation results for two main cases:

1. *Polymer melt dynamics*

   The simulated system is an ensemble of polymer chains placed in a cubic simulation box, with periodic boundary conditions.

2. *The debonding of two polymer bulks connected with connector chains*

   The simulated system consists of two simulation boxes on top of each other, with periodic boundary conditions in the directions perpendicular to the interface and with LJ-walls parallel to the interface. The connector chains are placed at the interface penetrating both simulation boxes.

In order to be able to enter the MD simulations, the polymer systems have to be initialized carefully. For this, three preparation steps are followed:

1. Generation of individual polymer chains/connectors. Different methods are used for specific types of chain stiffness.

2. Locating the bulk chains in random places inside the simulation box/boxes and packing them as uniformly as possible. The packing is done by MC 'moves' that perform a randomly chosen geometric transformation (chain translation, rotation

or reflection on a randomly chosen polymer chain until a desired homogeneity is reached). This packing method is a simplification of the method discussed by Auhl et al. (2003). Locating the connector chain in random places at the interface between boxes.

3. Pre-equilibrating the system by employing a capped WCA potential (cWCA) with the aim to eliminate the initial bead overlaps that can induce numerical instabilities:

$$V_{\mathrm{cWCA}}(r_{ij}) = \begin{cases} V_{\mathrm{WCA}}(r_{\mathrm{S}})\,, & r_{ij} < r_{\mathrm{S}} \\ V_{\mathrm{WCA}}(r_{ij})\,, & r_{ij} \geq r_{\mathrm{S}}\,. \end{cases} \tag{3.16}$$

i.e. the WCA force between two particles that are closer than a threshold distance r_{S} is replaced with the WCA force at this distance (see Fig. 3.8 for $r_{\mathrm{S}} = 1.0\sigma$). The particles that are further apart than the 'safe' distance are subjected to the full WCA force. In order to allow the beads to move apart easier, the bending and torsion potentials are turned off during this pre-equilibration stage.

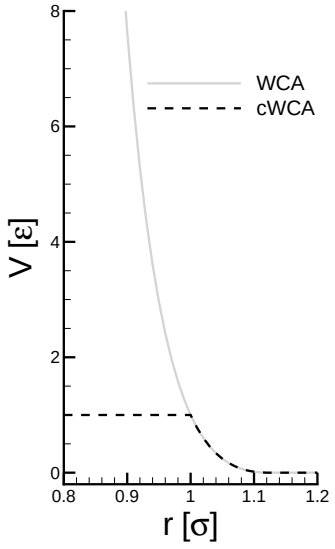

Figure 3.8: *"Capped" WCA interaction (cWCA) used instead of "full" interaction (WCA) to avoid instabilities when two beads would be too close to each other and would be repelled by colossal forces.*

This technique is a simplification of the "slow push off" method of Auhl et al. (2003) and guarantees a small perturbation of the chain configurations at the transition from modified to full WCA potential. The modified MD simulation is performed with this threshold WCA force until all beads are pushed away from the overlap regions. Then, the full WCA, bending and torsion potentials are turned-on and the main MD simulation can start.

3.9 Molecular dynamics computer program

For the simulation of polymeric materials (melt dynamics and adhesion fracture) we have developed a FORTRAN 77 classical molecular dynamics code that runs on single-processor machines. The code developed for this thesis is most similar with LAMMPS: Large-scale Atomic/Molecular Massively Parallel Simulator (Plimpton 1995) developed at Sandia National Laboratories.

A personal code was needed due to the specificity of the simulated systems and of the novelty of some force-field features. The simulated systems contain a relatively large number of particles (up to 1 million), the system initialization requires specific "tricks" of packing and pre-equilibration specific to dense polymer ensembles (cf. Sec. 3.8), the force field includes a novel torsion potential (cf. Sec. 3.4) and, last but not least, special polymeric architectures have to be build for the adhesion study (cf. Sec. 6.2.2).

For computational efficiency we use a linked-cell algorithm for building the Verlet list. In this way, the computing time dependence on the total number of particles M modifies from M^2 to M^1. The obtained average speed is 1.9×10^5 particle updates per second on a 2.8-GHZ/1-GB Pentium 4 processor (for melt simulations at $T = 1.0\varepsilon/k_{\mathrm{B}}$). Simulations have been carried out on multiple machines and on a HPC-Beowulf cluster (200 Opteron dual-processor nodes: 2(4)-GHz/1-GB memory). The results reported in this thesis are based on a total computation time of more than 10 CPU years.